



Published in final edited form as:

Biotechnol J. 2017 September ; 12(9): . doi:10.1002/biot.201600750.

Mechanotransduction Effects on Endothelial Cell Proliferation via CD31 and VEGFR2: Implications for Immunomagnetic Separation

Kalpesh D. Mahajan¹, Gauri M. Nabar¹, Wei Xue¹, Mirela Anghelina², Nicanor Moldovan³, Jeffrey Chalmers¹, and Jessica Winter^{1,4}

¹William G. Lowrie Department of Chemical and Biomolecular Engineering, The Ohio State University, Columbus, USA

²Department of Internal Medicine, Division of Hematology, The Ohio State University, Columbus, USA

³Davis Heart and Lung Research Institute, The Ohio State University, Columbus, USA

⁴Department of Biomedical Engineering, The Ohio State University, Columbus, USA

Abstract

Immunomagnetic separation is used to isolate circulating endothelial cells (ECs) and endothelial progenitor cells (EPCs) for diagnostics and tissue engineering. However, potentially detrimental changes in cell properties have been observed post-separation. Here, we studied the effect of mechanical force, which is naturally applied during immunomagnetic separation, on proliferation of human umbilical vein endothelial cells (HUVEC), kinase insert domain-positive receptor (KDR) cells, and peripheral blood mononuclear cells (PBMCs). Cells were exposed to CD31 or Vascular Endothelial Growth Factor Receptor-2 (VEGFR2) targeted MACSi beads at varying bead to cell ratios and compared to free antibody and unconjugated beads. A vertical magnetic gradient was applied to static 2D cultures, and a magnetic cell sorter was used to analyze cells in dynamic flow. No significant difference in EC proliferation was observed for controls or VEGFR2-targeting beads, whereas CD31-conjugated beads increased proliferation in a dose dependent manner in static 2-D cultures. This effect occurred in the absence of magnetic field, but was more pronounced with magnetic force. After flow sorting, similar increases in proliferation were seen for CD31 targeting beads. Thus, the effects of targeting antibody and magnetic force applied should be considered when designing immunomagnetic separation protocols for ECs.

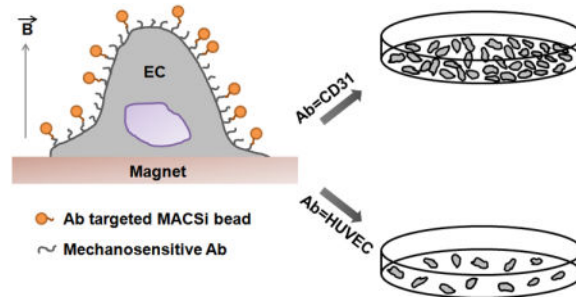
Graphical abstract

Magnetic beads are commonly conjugated to cell surface receptors for isolating cells from heterogeneous mixtures. We found that conjugating magnetic beads to cells via CD31 receptors using common immunomagnetic separation protocols increases cell proliferation, whereas VEGFR2 binding does not. These observations were confirmed using multiple cell types and by

Correspondence: Dr. Jessica O. Winter, William G. Lowrie Department of Chemical and Biomolecular Engineering, The Ohio State University, 151 West Woodruff Avenue, Columbus, OH 43210, USA. winter.63@osu.edu.

Conflict of interest: The authors declare no financial or commercial conflict of interest.

subjecting magnetic beads to different modes of magnetic field activation. Thus, caution must be exercised when selecting cell surface receptors targeted in immunomagnetic separation protocols to prevent unanticipated pathway activation in cells.



Keywords

cell separation; magnetic; mechanotransduction; endothelial cells

1. Introduction

Endothelial cells (ECs) are located at the interface between the blood and tissue parenchyma. ECs become activated in response to pathological conditions and can potentially be used as predictive indicators for a variety of conditions, including aging, atherosclerosis, heart failure, diabetes, hypertension, obesity [1], vascular injury and repair, neovascularization, and cancers [2]. Endothelial progenitor cells (EPCs) are a class of adult stem cells that can differentiate into ECs. EPCs support the maintenance of a functional endothelial layer and adult neovascularization [3, 4]. Because of their potential applications in cell therapy for heart [5], lung [6], and blood diseases [7], there is substantial interest in developing technologies that can isolate ECs and EPCs from blood and tissues for diagnostic and therapeutic applications.

Introduced by Jackson et al. [8], immunomagnetic separation is one of the most popular methods employed in EC separation. Using markers associated with the endothelial phenotype [9], this approach can be used for isolation of EPCs, ECs, human umbilical vein endothelial cells (HUVECs), and human blood outgrowth endothelial cells (HBOECs) from blood, tissue, and fat [8, 10]. However, potentially detrimental effects, such as reduction in cell proliferation following immunomagnetic cell isolation have been observed [11-13]. These reductions have been attributed to the lack of biocompatibility of the magnetic beads used in the separation process [11]. However, we hypothesized that these changes could result from chemical stimulation of the receptors used in separation via antibody binding, and that this effect could potentially be enhanced via application of magnetic force (i.e., mechanotransduction) during separation processes.

ECs are known to be mechanosensitive, which is not surprising given the complex mechanical environment in the vasculature. ECs are subjected to pulsatile flow and shear stresses, and use these cues to regulate blood pressure via release of soluble factors [14]. These forces have been shown to influence EC shape, with a tendency to align in the

direction of flow, and to alter proliferation, cell cycle regulation, and apoptotic response [14, 15]. Relevant to this work, proliferation increases in response to increased or disturbed flow [16-19] and is reduced in laminar conditions [20, 21]. Cyclic strain also influences proliferation, but responses are dictated by cell type and strain level [22, 23]. Increased proliferation is linked to sustained ERK signaling, suggesting possible mechano-regulation of this pathway. Several receptors have been implicated in these mechanotransduction responses, including integrins, tyrosine kinase receptors, g-protein coupled receptors, and cell adhesion molecules. In particular, Vascular Endothelial Growth Factor Receptor-2 (VEGFR2, KDR, Flk-1, CD309) and Platelet Endothelial Cell Adhesion Molecule-1 (PECAM-1, CD31) have been shown to play a central role in EC mechanotransduction [24, 25]. These responses are generally believed to be initiated by application of strain to a receptor, initiating a physical change in the protein that can yield hidden cryptic binding sites or change interactions with intracellular components [26]. It is thus reasonable that application of magnetic force could mimic the effects of shear flows, and indeed, magnetic force application is an accepted method of evaluating cellular mechanotransduction responses [27]. However, little attention has focused on the possible influence of induced mechanotransduction responses in magnetic cell separation procedures [28].

Here, we examined the biochemical effects of antibody binding and the biophysical results of force application via magnetic beads on VEGFR2 and CD31 receptors, which have been previously implicated in mechanotransduction [24, 25] and are routinely used in EC/EPC separation [29]. These effects were examined in three cell types: HUVECs, a common commercial type of ECs; 'KDR+' cells, which are human embryonic kidney cells (HEK293 line) that over-express VEGFR2; and peripheral blood monocytes (PBMCs), which contain more primitive circulating cells that can differentiate into other vascular cell types [30]. Cells interacted with magnetic beads commonly used in cell separation and were exposed to magnetic force application in two models. The first consisted of a magnetic plate capable of applying a vertical gradient to cells cultured in the system. The second consisted of a flow-through magnetic cell sorter, known as the 'quadrupole magnetic sorter', developed by Sun et al. [31]. In this device, the cells flow through an annular channel surrounded by a quadrupole magnet. The magnetically labelled cells are sequestered in the column, whereas the unlabeled, non-magnetic cells pass through. Shear stress resulting from the flow rate through the column reduces non-specific binding. Using these models, the influence of bead binding and force application on cell proliferation was explored.

2 Materials and methods

2.1 Cell Culture

HUVECs were purchased from Lonza (CC-2517) and cultured in Bulletkit medium prepared by mixing basal medium EBM@-2 (CC-3156, Lonza) with SingleQuots@ (CC-4133, Lonza) supplements and growth factors, including hydrocortisone, human epidermal growth factor (hEGF), fetal bovine serum (FBS), vascular endothelial growth factor (VEGF), human fibroblast growth factor basic (hFGFB), recombinant insulin growth factor-I, expressed in *E. coli*, (R3-IGF-I) ascorbic acid, heparin and gentamicin/amphotericin-B. KDR cells were purchased from SibTech, Inc. (Cat No. SBT021-293, SibTech) and were cultured in

Dulbecco's modified eagle medium (DMEM) with 10% FBS and 2 mM L-glutamine. PMBCs were obtained from the American Red Cross and used as received immediately. During the experimental observation period, cells were cultured in CFU-Hill liquid medium Endocult (Cat No. 05900, Stem Cell Technologies) prepared by mixing CFU-Hill basal medium with CFU-Hill proliferation Supplement.

2.2 Cell Proliferation Measurements

Cell proliferation was assessed using the CyQuant Cell proliferation assay [32], which is based on the fluorescence intensity enhancement of CyQuant GR dye in response to binding cellular nucleic acids. As per manufacturer's instructions, frozen cells were thawed and lysed using cell lysis buffer. Dye was then added; and the enhancement in fluorescence was measured using a fluorescence microplate reader (Victor X, Perkin Elmer) with 480 nm excitation and 520 nm emission. Cell numbers were determined by comparison to a calibration curve generated for concentrations of 50 to 50,000 cells in a fixed volume. Calibration curves were considered acceptable if they displayed a correlation coefficient 0.99.

2.3 Antibody Conjugation to Magnetic Particles

Anti-Biotin MACSi bead particles (Cat No. 130-092-357, Miltenyi Biotec) were conjugated with Biotinylated CD309 (VEGFR2/KDR) (Cat No. 130-093-603, Miltenyi Biotec) or CD31 (Cat No. MA1-19510, Thermo Scientific Pierce Antibodies) antibodies through avidin-biotin interactions. Briefly, 10 μ l anti-biotin MACSi bead particles were added to 200 μ l of blocking buffer (5% bovine serum albumin (BSA) in phosphate buffered saline (PBS)) and incubated for 30 minutes at room temperature. Beads were then separated using a Magna-Sep magnetic separator (Cat No. K1585-01, Invitrogen) for 5 minutes. The supernatant was removed and 200 μ l of blocking buffer (0.5% BSA in PBS with 2 mM ethylenediaminetetraacetic acid(EDTA)) was added. Thirty μ g total biotinylated antibody was loaded per 10^8 beads and incubated for 2 hours at 2-8 $^{\circ}$ C under constant gentle rotation. Fifty μ l of this bead suspension was then added to 500 μ l medium and separated again using the Magna-Sep column. Beads conjugated with antibodies were then resuspended in fresh medium. For the control treated with free antibody, the amount of antibody present on the conjugated beads at the 20:1 bead to cell ratio was determined (assuming 100% conjugation efficiency), and an equivalent amount was added to solution.

2.4 Mechanotransduction Experiments

Three cell types (HUVEC, KDR, and PBMC) and two antibodies (VEGFR2 and CD31) were used in this study. For static 2D cultures, cells were loaded with magnetic beads at bead to cell ratios of 2, 5, 10, and 20 by incubation for 2 hours under gentle rotation. [Except that CD31 binding was not assessed in KDR cells as these do not express these receptors.] Cells were then washed with PBS and seeded in 96 well plates at a density of 5000 cells/well. As controls, cells were also exposed to free antibody and to unconjugated magnetic beads at the bead to cell ratio 20 concentrations. The effect of conjugated magnetic bead binding in the absence of a magnetic field was also assessed.

In the 2D static culture model, for each experiment, all treatment groups were seeded in two 96 well plates, one of which was subjected to magnetic force by placing it on a strong permanent magnet platform (Cat No. 2501008-1, Dexter Magnetic). The Dexter Magnetic platform provides a magnetic gradient primarily in the vertical direction. The other plate served as a control and was not subjected to magnetic force. Both plates were kept in an incubator at 37° C and cells were allowed to proliferate for 2.5 days. All experiments were conducted in triplicate.

To evaluate potential mechanotransduction effects induced during sorting, cells were processed using a permanent magnet cell sorter [31]. The cell suspension passed through the column in less than 1 minute. Magnetically labelled cells (bead to cell ratio 20:1) were retained in the column, whereas unlabeled cells flowed through. As a control, unlabeled cells were passed through the cell sorter. After collection, cells were cultured in 96 well plates for 2.5 days at a predetermined density (5000 cells/ml) to permit evaluation of effects resulting from magnetic exposure.

2.5 Statistics

All the statistical analyses were performed using JMP Pro 12 software (SAS Institute Inc., Cary, NC, USA). ANOVA was used to determine the effect of free antibody, unconjugated beads, and targeted beads at different bead to cell ratios on cell proliferation. P-values of <0.05 were interpreted as statistically significant.

3 Results

3.1 Bead Attachment to Cells

To examine the potential of chemical or physical activation of VEGFR2 and CD31 receptors, we employed MACSi beads (Miltenyi) commonly used in magnetic cell separation. These MACSi beads had an anti-biotin coating allowing conjugation with biotinylated antibodies and were of cell culture grade. These beads ($1.5 \mu\text{m} \pm 0.6 \mu\text{m}$) consist of multiple ~ 50 nm superparamagnetic nanoparticles encased in a biodegradable matrix, and are modified with avidin to permit conjugation to biotinylated antibodies. Beads were thus conjugated to antibodies targeting VEGFR2 and CD31 cell surface receptors via avidin-biotin interactions Figure 1(A, B). Before evaluating the response of cells to magnetic beads, we first examined the relationship between bead to cell ratio and cellular distribution. Irregular loading could lead to inhomogeneity in cell activation, which can display spatial variations [33]. As a model system, we first evaluated these effects using HUVECs. Bead distribution was not effected by magnetic treatment, and was non-uniform at lower bead to cell ratios. However, bead distribution became more uniform as bead to cell ratio was increased. Bead loading, which was measured by microscopic observation, was proportional to the bead to cell incubation ratio Figure 1(C), indicating that experimental conditions employed in this study were below saturation levels. Also, very little endocytosis was observed.

3.2 Effect of Unconjugated Beads and Free Antibody on Cell Proliferation

It has been suggested that decreases in cell proliferation observed in conjunction with immunomagnetic separation can be attributed to toxicity of the magnetic beads employed [11]. However, it is also possible that receptor activation/deactivation could result from antibody-receptor binding or from mechanical activation of those receptors [19]. To investigate the first two possibilities, the influence of free anti-VEGFR2 and anti-CD31 antibodies and unconjugated magnetic beads on HUVEC proliferation was examined in the absence of a magnetic field (Figure 2). Beads were added at a bead to cell ratio of 20, and antibodies were added at a concentration consistent with that experimentally determined to be present on beads at the highest ratio employed (i.e., 20). No statistically significant effect was observed, suggesting that the MACSi beads used in this study do not induce toxicity in the form of reduced EC proliferation for up to 2.5 days. This is in contrast to previous studies, which observed a significant dose dependent effect of bead toxicity on cell proliferation, particularly for long incubation times (6 days) [11], and detrimental effects on cell metabolism [12]. In addition, these results suggest that the antibodies employed in this study do not activate/deactivate VEGFR2 or CD31 receptors at the concentration employed.

3.3 Mechanotransduction Responses via VEGFR2 and CD31 in ECs in Static 2-D Culture

To determine the potential for magnetic force to induce mechanical activation of VEGFR2 and CD31 in ECs, mechanical force application via antibody-conjugated MACSi beads was examined. As a first approach, application of a magnetic gradient in a 2D culture system was evaluated. HUVEC proliferation was not affected by VEGFR2 conjugated beads in the absence of presence of magnetic field over 2.5 days (Figure 3). To confirm this result, we next examined VEGFR2 activation in KDR cells, which overexpress this receptor. Cell proliferation was not affected by VEGFR2 targeted beads. Thus, neither chemical binding nor magnetic force had a significant effect on cell proliferation through VEGFR2.

In contrast, a statistically significant, dose dependent increase in cell proliferation was observed for ECs exposed to CD31-targeting beads in the presence ($p=0.0003$) or absence ($p<0.0001$) of a magnetic field ($\alpha=0.05$). Proliferation increased for bead to cell ratios up to 10, but no further increases were observed at higher bead to cell ratios, suggesting a possible saturation response. Noting that proliferation did not increase after exposure to free CD31 antibody (Figure 2), proliferation increases for CD31-conjugated beads in the absence of a magnetic field most likely result from either a concentration effect or receptor clustering induced by MACSi bead binding. The concentration effect, which has previously been observed in similar systems [34], occurs because beads can present a higher antibody density to cells versus free antibody in solution, increasing effective concentration at the cell surface. Alternatively, it has also been shown that bead binding can initiate receptor aggregation [35], an effect that is more pronounced in the presence of a magnetic field.

Increases in proliferation in response to CD31 bead-binding were more pronounced with magnetic field application, and increased with increasing bead to cell ratio until a saturation point. Increased proliferation could occur because of attractive forces between beads, inducing receptor clustering. However, the potential influence of mechanical forces cannot

be neglected. Micron-sized magnetic beads, such as those employed here, have been shown capable of initiating mechanotransduction responses through their bound receptors [36].

These data suggest that VEGFR2 may be an appropriate receptor for isolation of ECs/EPCs as bead to cell ratio can be increased without unwanted effects (e.g., on cell proliferation) through either chemical or mechanical pathways. However, CD31 beads should be used with caution as it may increase cell proliferation, and could potentially also initiate additional cell responses that may alter function in their intended use. If increased cell proliferation is desired, a bead to cell ratio of 10 was optimal; however, no adverse effects were observed for bead to cell ratios up to 20. It is noted that higher ratios may be desired for immunomagnetic separations to yield more homogenous separations. Bead to cell ratios as high as 50 have been reported with similar bead products [11].

3.4 Mechanotransduction Responses via VEGFR2 and CD31 in ECs in Flow-based Cell Sorters

Next, we evaluated whether these results would translate to flow through separation systems, which may expose cells to larger forces, but for a shorter duration. Thus, cells labeled with beads at a 20:1 ratio were separated using a pre-commercial magnetic flow through sorter [37, 38]. Cells were exposed to magnetic force upon passage through the fractionation column. Cells labeled with magnetic beads were retained in the column, whereas non-labeled cells flowed through the device. After the entire cell suspension had passed through, the column was flushed with buffer to recover the magnetically-labeled cells. The total exposure time to magnetic force was less than a minute. The recovered cells were then cultured in 96 well plates for 2.5 days, and proliferation evaluated. These results were compared to controls experiencing no magnetic force and static 2D cultures exposed to magnetic gradients (bead to cell ratio 20:1). As expected, cells conjugated to VEGFR2-targeting beads displayed no difference in proliferation after magnetic cell sorting (Figure 4), as in 2D culture. Cells exposed to CD31-targeting beads and passed through the magnetic flow through sorter displayed increases in proliferation. These increases were statistically identical to those experienced following 2D plate exposure.

To further explore the influence of exposure time on proliferation, we subjected Peripheral Blood Mononuclear Cells (PBMCs) to magnetic gradients in 2D culture and using the flow through sorter at a 20:1 bead to cell ratio. PBMCs, contain both mononuclear leukocytes (monocytes and lymphocytes), but also a small fraction of more primitive cells. These are an important cell type for regenerative medicine, as they can potentially differentiate into other functional cells such as, endothelial [39], blood [30], bone [40], or neural cells [41]. Thus, high yield isolation of those progenitors from PBMC preparations is pivotal for development of cellular therapies. Some of them express VEGFR2 [42], but the majority express CD31, a homotypic molecule involved in their passing across an endothelial layer [43]. Similar to the HUVECs, no increases in proliferation were observed for VEGFR2-targeting beads, whereas CD31-targeted beads increased PMBC proliferation for both exposure methods (Figure 4). Increases in proliferation were statistically indistinguishable for HUVECs and PMBCs.

3.5 Estimating Maximum Force Applied Via MACSi Beads

To further compare 2D plate culture to magnetic flow through sorting, the maximum possible force applied via each method was determined. First, the magnetic susceptibility of MACSi beads was experimentally determined by measuring their magnetophoretic mobility (i.e., the velocity resulting from the magnetic force acting on the cell) using the protocol described by Nakamura et al. [44]. Beads were introduced into an electromagnet cell tracking velocimetry (eCTV) instrument at a concentration of 2×10^8 beads/mL in phosphate buffer saline (PBS). Beads were subjected to a well characterized and uniform magnetic gradient [44]. The horizontal velocity of the beads induced by the magnetic field (u_m) was recorded and analyzed. Magnetophoretic mobility (m) was calculated by dividing the horizontal velocity of the beads (u_m , Eqn. 1) by the magnetic energy gradient (S_m , Eqn. 2).

$$u_m = m \cdot S_m \quad (1)$$

$$S_m = \frac{B}{\mu_o} \left(\frac{\partial B}{\partial x} \right) \quad (2)$$

In this experiment, a total electric current of 0.2 A was applied, and therefore the applied magnetic field, B , was equal to 0.1013 T and the magnetic energy density gradient, S_m , was equal to 0.8356 T-A/mm². These values were then used to determine the average magnetophoretic mobility by solving equations (1) and (2) at different time points, resulting in an average value of $m = 6.9 \times 10^{-11}$ m³/T-A-s. The magnetization of the particle, M_p (A/m) at the field B (T) is related to the magnetophoretic mobility, m , by [45]:

$$m = \frac{\left(\frac{\mu_o M_p}{B} - \chi_F \right) D_p^2}{18\eta} \quad (3)$$

where, μ_o is the magnetic field permeability in free space equal to 1.23×10^{-6} m kg s⁻² A⁻², χ_F is the magnetic susceptibility of PBS (approximated as water) by volume equal to -9.035×10^{-6} , D_p is mean bead diameter, and η is viscosity of PBS equal to 10^{-3} Pa-s at room temperature. The mean diameter of MACSi beads was measured via an Olympus IX71 upright brightfield microscope and evaluated using Image-J analysis software as $1.5 \mu\text{m} \pm 0.6 \mu\text{m}$. Substituting these values into Eqn. 3 yields a MACSi bead magnetization (M_p) of 4.45×10^4 A/m. Because MACSi beads are composed of superparamagnetic iron oxide nanoparticles and a polymer support matrix, the magnetization results from the iron oxide content only. According to the magnetization versus applied field profile for these particles [45], at the applied magnetic field of 0.1 T, the magnetization is $\sim 77.8\%$ saturated. Hence the saturated magnetization, $M_S = M_p/77.8\%$, is 5.69×10^4 A/m.

The magnetic force experienced by a MACSi bead is the result of bead interaction with an external magnetic field and is given by:

$$F_m = M_s V_p \nabla B \quad (4)$$

where M_s is the saturated magnetization of the particle equal to 5.69×10^4 A/m (as calculated above) and V_p is the average MACSi bead volume equal to 1.77×10^{-18} m³. Substituting M_s and V_p into Eqn. 4 yields:

$$F_m = 10^{-13} \nabla B \quad (5)$$

Thus, if ∇B is known, the applied force per bead can be determined. The magnetic field density, perpendicular to the Dexter magnetic platform, was measured at specific, regular intervals using a gaussmeter. This data was used to determine the gradient present (Figure 5). The gradient of the quadrupole flow through sorter has been determined previously [31]. Substituting these magnetic field gradients into Eqn. 5 yields the magnitude of the maximum magnetic force acting on the MACSi beads (Table 1). These forces exceed the range previously reported to induce mechanical activation of these receptors (~ 20 pN, ~ 2.5 dyne/cm²) [46, 47].

4 Discussion

The primary goal of this work was to examine the potential mechanical activation of receptors used in the magnetic separation of blood cells during the separation process. In this study, we examined the effect of MACSi bead binding during immunomagnetic separation on HUVEC, KDR cell, and PBMC proliferation using antibodies targeting two potentially mechanosensitive receptors (VEGFR2, CD31) and 2 magnetic platforms (static 2D culture and flow through sorter). We determined that unconjugated beads did not alter EC proliferation, suggesting that toxicity was not a cause for any subsequently observed changes in cell proliferation at the concentrations investigated. Further, proliferation did not increase upon exposure to free antibody binding for either antibody investigated. VEGFR2-targeted MACSi beads did not affect proliferation in any system investigated, suggesting that this may be an appropriate receptor for EC isolation. In contrast, CD31 targeted MACSi beads produced a dose-dependent enhancement in HUVEC proliferation in static 2-D culture, and also increased proliferation in flow through systems.

Although mechanistic study of these two receptors was not the goal of this study, the lack of response to VEGFR2-targeting beads is consistent with current knowledge of VEGFR2 mechanotransduction response. Mechanotransduction in VEGFR2 can be initiated through shear stress, even in the absence of chemical binding [47]. Thus, it is not surprising that chemical activation by antibody binding alone failed to elicit a response. Further, although shear stress increases VEGFR2 expression and activates its phosphorylation, these changes can be transient. Increases in expression can disappear within as few as 30 minutes of

continuous stress application [48], providing one possible explanation for the lack of observed mechanotransduction response at 2.5 days.

Further, EC/EPC proliferation has been shown to increase through mechanical activation of PI3K and downstream ERK-dependent pathways [19, 47]. However, mechanically induced changes in VEGFR2 expression are regulated by PI3K, but not ERK inhibitors. In contrast, during EC stimulation through shear stress, CD31 undergoes tyrosine phosphorylation [49] that activates the ERK pathway [24]. This suggests that ERK activation is a key step in increasing EC proliferation, and future molecular studies of this pathway are recommended to confirm this hypothesis. Activation of this pathway may be initiated chemically. Although we did not observe increased proliferation in the presence of free antibody, a concentration effect may have generated this response when antibody-conjugated beads were presented to cells [34]. In addition, it is possible that proliferation increased via bead-induced aggregation, which was more pronounced in a magnetic field. Nonetheless, the fact that responses were increased with magnetic field exposure provides clear evidence for mechanical activation of this pathway through direct force application or receptor clustering. The MACSi beads employed in this experiment experienced approximately 17 pN of magnetic force. It has been shown that forces of this magnitude can deform the cell membrane and activate nearby mechanosensitive ion channels [50].

Importantly, these increases in proliferation in response to CD31 targeted beads were observed for both static 2D culture and flow through magnetic systems, suggesting that activation results not only from exposure to static gradients as would be expected from prior literature [24, 25], but can also occur during magnetic separation processes. The magnitude of the maximum magnetic force acting on the MACSi beads is higher for the flow sorter; however, the duration of exposure is several orders of magnitude smaller (< 1 min vs. 2.5 days). CD31 phosphorylation has been shown in mechanically stimulated cells within 30 seconds of force exposure [46, 49]. However, we cannot rule out the possibility of activation via shear forces, which are also present in the flow through system.

CD31 activation induced by magnetic cell separation has many potential implications for downstream users. Mechanical force results in CD31 phosphorylation via src kinase. Because phosphorylation can occur in < 1 min [46, 49] even short exposures to magnetic gradients may initiate a response. Once activated, CD31 signaling is associated with increases in cytoskeletal stiffness and focal adhesion assembly via actin reorganization, which are modulated through PI3K. CD31 mechanical stimulation also activates the RhoA pathway, and these responses are global, not localized to the point of activation [51]. Additionally, CD31 activation is associated with regulation of the β_1 integrin, all of which suggest a potential role in adhesion and migration. CD31 has also been shown to promote cell survival [52]. Thus, forces applied during magnetic separation processes have the potential to initiate a cascade of CD31-mediated responses, promoting cell adhesion, migration, and survival. These data suggest that magnetic force applied via beads should be considered when designing protocols for immunomagnetic EC separations.

Acknowledgments

The authors gratefully acknowledge the support of NIH 1RC2AG036559-01 and NIH R01 CA062349-15.

References

1. Hunting CB, Noort WA, Zwaginga JJ. Circulating endothelial (progenitor) cells reflect the state of the endothelium: vascular injury, repair and neovascularization. *Vox Sang.* 2005; 88:1–9. [PubMed: 15663716]
2. Mancuso P, Burlini A, Pruneri G, Goldhirsch A, et al. Resting and activated endothelial cells are increased in the peripheral blood of cancer patients. *Blood.* 2001; 97:3658–3661. [PubMed: 11369666]
3. Asahara T, Masuda H, Takahashi T, Kalka C, et al. Bone Marrow Origin of Endothelial Progenitor Cells Responsible for Postnatal Vasculogenesis in Physiological and Pathological Neovascularization. *Circ Res.* 1999; 85:221–228. [PubMed: 10436164]
4. Tepper OM, Capla JM, Galiano RD, Ceradini DJ, et al. Adult vasculogenesis occurs through in situ recruitment, proliferation, and tubulization of circulating bone marrow-derived cells. *Blood.* 2005; 105:1068–1077. [PubMed: 15388583]
5. Grisar JC, Haddad F, Gomari FA, Wu JC. Endothelial progenitor cells in cardiovascular disease and chronic inflammation: from biomarker to therapeutic agent. *Biomark Med.* 2011; 5:731–744. [PubMed: 22103609]
6. Lee JH, Bhang DH, Beede A, Huang TL, et al. Lung Stem Cell Differentiation in Mice Directed by Endothelial Cells via a BMP4-NFATc1-Thrombospondin-1 Axis. *Cell.* 2014; 156:440–455. [PubMed: 24485453]
7. Solovey AA, Solovey AN, Harkness J, Hebbel RP. Modulation of endothelial cell activation in sickle cell disease: a pilot study. *Blood.* 2001; 97:1937–1941. [PubMed: 11264155]
8. Jackson CJ, Garbett PK, Nissen B, Schrieber L. Binding of human endothelium to *Ulex europaeus* I-coated Dynabeads: application to the isolation of microvascular endothelium. *J Cell Sci.* 1990; 96:257–262. [PubMed: 2211866]
9. Brunner S, Schernthaner GH, Satler M, Elhenicky M, et al. Correlation of different circulating endothelial progenitor cells to stages of diabetic retinopathy: first in vivo data. *Invest Ophthalmol Vis Sci.* 2009; 50:392–398. [PubMed: 18719083]
10. Hewett P, Murray J. Human microvessel endothelial cells: Isolation, culture and characterization. *In Vitro Cellular & Developmental Biology - Animal.* 1993; 29:823–830.
11. Tiwari A, Punshon G, Kidane A, Hamilton G, Seifalian AM. Magnetic beads (Dynabead™) toxicity to endothelial cells at high bead concentration: Implication for tissue engineering of vascular prosthesis. *Cell Biol Toxicol.* 2003; 19:265–272. [PubMed: 14703114]
12. Conrad-Lapostolle V, Bordenave L, Baquay C. Optimization of use of UEA-1 magnetic beads for endothelial cell isolation. *Cell Biol Toxicol.* 1996; 12:189–197. [PubMed: 9034608]
13. Higgins DA, Ko WKW. Duck lymphocytes. VII. Selection of subpopulations using lectin-coated magnetic beads. *Vet Immunol Immunopathol.* 1995; 44:181–195. [PubMed: 7747400]
14. Ando J, Yamamoto K. Effects of Shear Stress and Stretch on Endothelial Function. *Antioxid Redox Signal.* 2010; 15:1389–1403.
15. Hahn C, Schwartz MA. Mechanotransduction in vascular physiology and atherogenesis. *Nat Rev Mol Cell Biol.* 2009; 10:53–62. [PubMed: 19197332]
16. Masuda H, Kawamura K, Tohda K, Shozawa T, et al. Increase in Endothelial-Cell Density Before Artery Enlargement in Flow-Loaded Canine Carotid-Artery. *Arteriosclerosis.* 1989; 9:812–823. [PubMed: 2590062]
17. Davies PF, Remuzzi A, Gordon EJ, Dewey CF, Gimbrone MA. Turbulent Fluid Shear-Stress Induces Vascular Endothelial-Cell Turnover In Vitro. *Proc Natl Acad Sci U S A.* 1986; 83:2114–2117. [PubMed: 3457378]
18. Brooks AR, Lelkes PI, Rubanyi GM. Gene expression profiling of vascular endothelial cells exposed to fluid mechanical forces: Relevance for focal susceptibility to atherosclerosis. *Endothelium-Journal of Endothelial Cell Research.* 2004; 11:45–57. [PubMed: 15203878]

19. Li YSJ, Haga JH, Chien S. Molecular basis of the effects of shear stress on vascular endothelial cells. *J Biomech.* 2005; 38:1949–1971. [PubMed: 16084198]
20. Akimoto S, Mitsumata M, Sasaguri T, Yoshida Y. Laminar shear stress inhibits vascular endothelial cell proliferation by inducing cyclin-dependent kinase inhibitor p21(Sdi1/Cip1/Waf1). *Circ Res.* 2000; 86:185–190. [PubMed: 10666414]
21. Cunningham KS, Gotlieb AI. The role of shear stress in the pathogenesis of atherosclerosis. *Lab Invest.* 2005; 85:9–23. [PubMed: 15568038]
22. Woodell JE, LaBerge M, Langan EM, Hilderman, R. H., In vitro strain-induced endothelial cell dysfunction determined by DNA synthesis. *Proceedings of the Institution of Mechanical Engineers Part H-Journal of Engineering in Medicine.* 2003; 217:13–20.
23. Sumpio BE, Banes AJ, Levin LG, Johnson G. Mechanical-Stress Stimulates Aortic Endothelial-Cells To Proliferate. *J Vasc Surg.* 1987; 6:252–256. [PubMed: 3625881]
24. Fujiwara K. Platelet endothelial cell adhesion molecule-1 and mechanotransduction in vascular endothelial cells. *J Intern Med.* 2006; 259:373–380. [PubMed: 16594905]
25. Tzima E, Irani-Tehrani M, Kiosses WB, Dejana E, et al. A mechanosensory complex that mediates the endothelial cell response to fluid shear stress. *Nature.* 2005; 437:426–431. [PubMed: 16163360]
26. Bao, G. Protein conformational change: A molecular basis of mechanotransduction. In: Mofrad, MRK., Kamm, RD., editors. *Cellular Mechanotransduction: diverse perspective from molecules to tissues.* Cambridge University Press; New York: 2010. p. 269-285.
27. Lele TP, Sero JE, Matthews BD, Kumar S, et al. Tools to study cell mechanics and mechanotransduction. *Methods Cell Biol.* 2007; 83:443–472. [PubMed: 17613320]
28. Bharde AA, Palankar R, Fritsch C, Klaver A, et al. Magnetic Nanoparticles as Mediators of Ligand-Free Activation of EGFR Signaling. *PLoS One.* 2013; 8
29. Boos CJ, Lip GYH, Blann AD. Circulating Endothelial Cells in Cardiovascular Disease. *J Am Coll Cardiol.* 2006; 48:1538–1547. [PubMed: 17045885]
30. Zhang M, Huang B. The multi-differentiation potential of peripheral blood mononuclear cells. *Stem Cell Research & Therapy.* 2012; 3
31. Sun L, Zborowski M, Moore LR, Chalmers JJ. Continuous, flow-through immunomagnetic cell sorting in a quadrupole field. *Cytometry.* 1998; 33:469–475. [PubMed: 9845442]
32. Jones LJ, Gray M, Yue ST, Haugland RP, Singer VL. Sensitive determination of cell number using the CyQUANT cell proliferation assay. *J Immunol Methods.* 2001; 254:85–98. [PubMed: 11406155]
33. Simons M, Gordon E, Claesson-Welsh L. Mechanisms and regulation of endothelial VEGF receptor signalling. *Nat Rev Mol Cell Biol.* 2016; 17:611–625. [PubMed: 27461391]
34. Luo D, Saltzman WM. Enhancement of transfection by physical concentration of DNA at the cell surface. *Nat Biotechnol.* 2000; 18:893–895. [PubMed: 10932162]
35. Perica K, Tu A, Richter A, Bieler JG, et al. Magnetic Field-Induced T Cell Receptor Clustering by Nanoparticles Enhances T Cell Activation and Stimulates Antitumor Activity. *Acs Nano.* 2014; 8:2252–2260. [PubMed: 24564881]
36. Dobson J. Remote control of cellular behaviour with magnetic nanoparticles. *Nature Nanotechnology.* 2008; 3:139–143.
37. Yang L, L JC, Balasubramanian P, Jatana KR, Schuller D, Agrawal A, Zborowski M, Chalmers JJ. Optimization of an enrichment process for circulating tumor cells from blood of head and neck cancer patients through depletion of normal cells. *Biotechnol Bioeng.* 2009; 102:521–534. [PubMed: 18726961]
38. Zborowski M, Chalmers JJ. Rare Cell Separation and Analysis by Magnetic Sorting. *Anal Chem.* 2011
39. Korbling M, Katz RL, Khanna A, Ruifrok AC, et al. Hepatocytes and epithelial cells of donor origin in recipients of peripheral-blood stem cells. *N Engl J Med.* 2002; 346:738–746. [PubMed: 11882729]
40. Wan C, He QL, Li G. Allogenic peripheral blood derived mesenchymal stem cells (MSCs) enhance bone regeneration in rabbit ulna critical-sized bone defect model. *J Orthop Res.* 2006; 24:610–618. [PubMed: 16514623]

41. Kim S, Honmou O, Kato K, Nonaka T, et al. Neural differentiation potential of peripheral blood- and bone-marrow-derived precursor cells. *Brain Res.* 2006; 1123:27–33. [PubMed: 17064670]
42. Walenta K, Friedrich EB, Sehnert F, Werner N, Nickenig G. In vitro differentiation characteristics of cultured human mononuclear cells - implications for endothelial progenitor cell-biology. *Biochem Biophys Res Commun.* 2005; 333:476–482. [PubMed: 15961064]
43. Muller WA. Localized signals that regulate transendothelial migration. *Curr Opin Immunol.* 2016; 38:24–29. [PubMed: 26584476]
44. Nakamura M, Zborowski M, Lasky LC, Margel S, Chalmers JJ. Springer-Verlag. 2001:371–380.
45. Xu J, Mahajan KD, Xue W, Winter JO, et al. Simultaneous, single particle, magnetization and size measurements of micron sized, magnetic particles. *J Magn Magn Mater.* 2012; 324:4189–4199. [PubMed: 22962515]
46. Osawa M, Masuda M, Kusano K, Fujiwara K. Evidence for a role of platelet endothelial cell adhesion molecule-1 in endothelial cell mechanosignal transduction: is it a mechanoresponsive molecule? *J Cell Biol.* 2002; 158:773–785. [PubMed: 12177047]
47. Obi S, Masuda H, Shizuno T, Sato A, et al. Fluid shear stress induces differentiation of circulating phenotype endothelial progenitor cells. *American Journal of Physiology-Cell Physiology.* 2012; 303:C595–C606. [PubMed: 22744008]
48. Chen KD, Li YS, Kim M, Li S, et al. Mechanotransduction in response to shear stress - Roles of receptor tyrosine kinases, integrins, and Shc. *J Biol Chem.* 1999; 274:18393–18400. [PubMed: 10373445]
49. Osawa M, Masuda M, Harada N, Lopes RB, Fujiwara K. Tyrosine phosphorylation of platelet endothelial cell adhesion molecule-1 (PECAM-1, CD31) in mechanically stimulated vascular endothelial cells. *Eur J Cell Biol.* 1997; 72:229–237. [PubMed: 9084985]
50. Ingber DE. From Cellular Mechanotransduction to Biologically Inspired Engineering. *Annals of Biomedical Engineering.* 2010; 38:1148–1161. [PubMed: 20140519]
51. Collins C, Guilluy C, Welch C, O'Brien ET, et al. Localized Tensional Forces on PECAM-1 Elicit a Global Mechanotransduction Response via the Integrin-RhoA Pathway. *Current Biology.* 2012; 22:2087–2094. [PubMed: 23084990]
52. Newman PJ, Newman DK. Signal transduction pathways mediated by PECAM-1 - New roles for an old molecule in platelet and vascular cell biology. *Arteriosclerosis Thrombosis and Vascular Biology.* 2003; 23:953–964.

Abbreviations

BSA	bovine serum albumin
DMEM	Dulbecco's modified eagle medium
ECs	endothelial cells
eCTV	electromagnet cell tracking velocimetry
EPCs	endothelial progenitor cells
ERK	extracellular regulated kinase
FBS	fetal bovine serum
HBOECs	human blood outgrowth endothelial cells
hEGF	human epidermal growth factor
hFGFB	human fibroblast growth factor basic
HUVECs	human umbilical vein endothelial cells

KDR	kinase insert domain-positive receptor
PBMCs	peripheral blood monocytes
PBS	phosphate buffered saline
PECAM-1	Platelet Endothelial Cell Adhesion Molecule-1
PI3K	Phosphoinositide 3-kinase
R3-IGF-I	recombinant insulin growth factor-I
VEGF	vascular endothelial growth factor
VEGFR2	vascular endothelial growth factor receptor 2

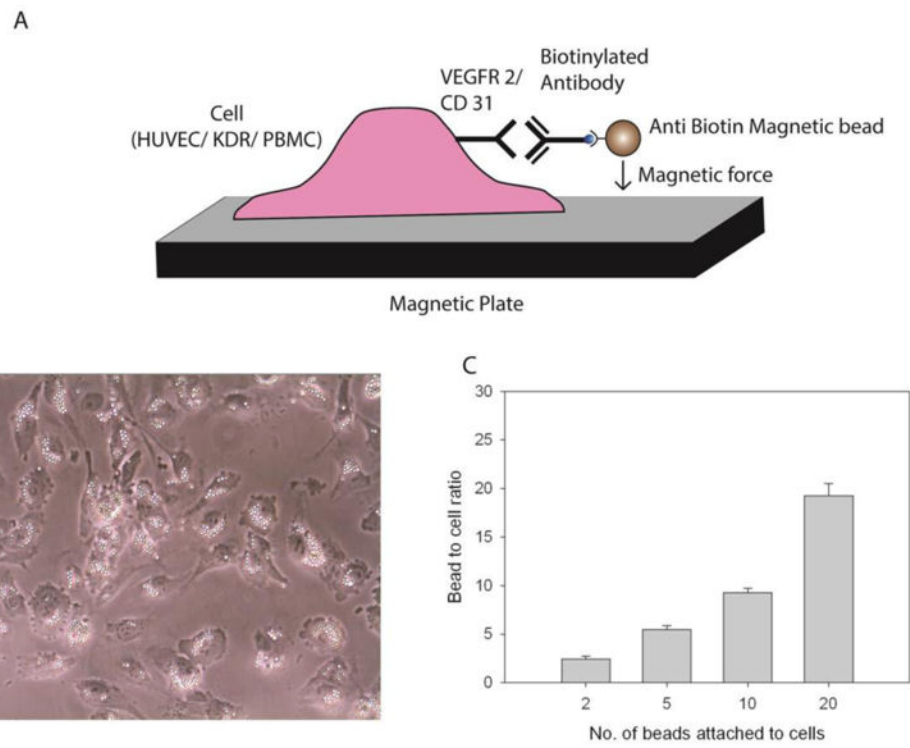


Figure 1. Magnetic bead conjugation to cells (**A**) Schematic, (**B**) microscope image of anti-CD31 MACSi beads attached to HUVECs, (**C**) Number of beads attached to HUVECs as a function of bead to cell ratio (anti-CD31 beads shown).

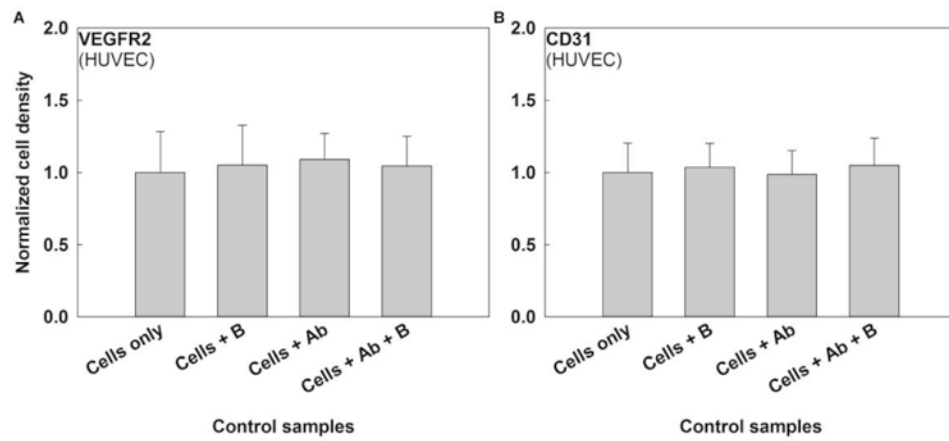


Figure 2. Effects of unconjugated beads (B) and free antibody (Ab) on HUVEC proliferation for (A) VEGFR2 and (B) CD31 antibodies. No statistically significant difference in cell proliferation was observed following exposure to unconjugated beads, antibodies, or their combination at a significance level $\alpha=0.05$. Starting sample size=10,000 cells, $N = 3$ for each setting.

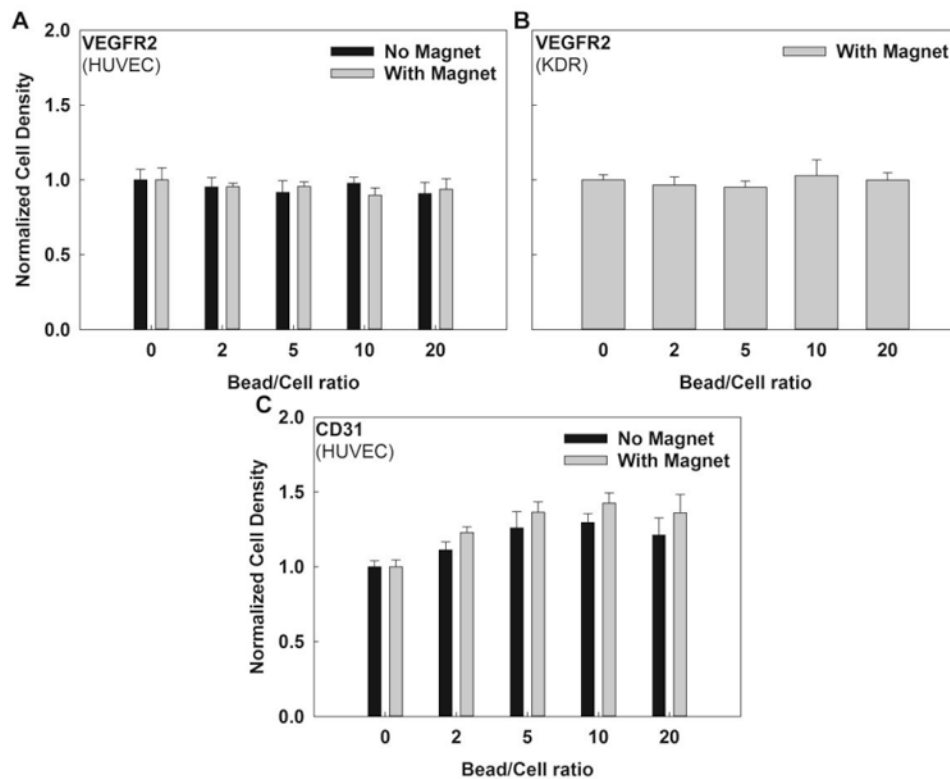


Figure 3.

Cell proliferation in 2D culture versus bead to cell ratio in the absence or presence of a magnetic field for (A) VEGFR2 targeting beads exposed to HUVECs, (B) VEGFR2 targeting beads exposed to KDR cells. No statistically significant differences were seen in the cell proliferation of HUVECs or KDR cells conjugated with VEGFR2 targeting beads. (C) CD31 targeting beads exposed to HUVECs. There was a statistically significant difference in cell proliferation of HUVECs conjugated with CD31 targeting beads in the absence or presence of magnetic field ($p < 0.0001$). Further, there was a statistically significant difference in cell proliferation with increasing bead to cell ratio for HUVECs exposed to CD31-targeting beads in the presence ($p = 0.0003$) or the absence ($p < 0.0001$) of a magnetic field ($\alpha = 0.05$). Starting sample size = 10,000 cells, $N = 3$ for each setting.

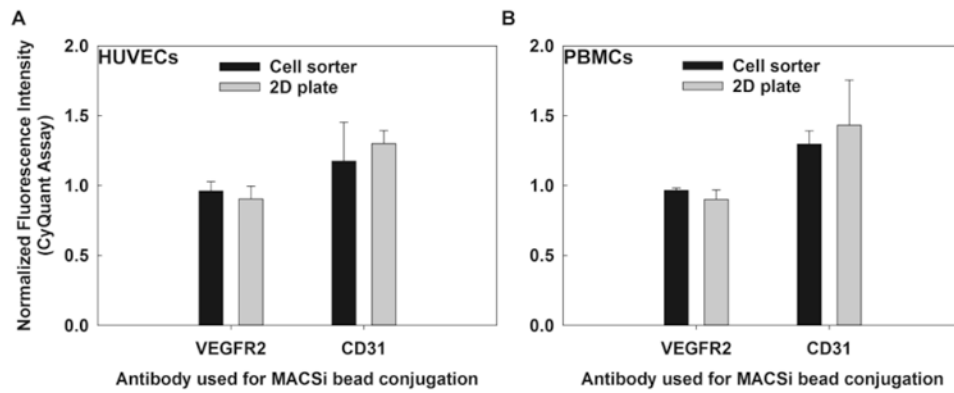


Figure 4. PBMC and HUVEC proliferation (CyQuant assay fluorescence intensity, normalized to control = 1) exposed to VEGFR2 targeting or CD31-targeting beads via a magnetic flow through sorter (short exposure) or a 2D permanent magnetic platform (long exposure): (A) HUVECs, (B) PBMCs. No statistical differences in proliferation were observed between the cell sorter and the 2D plate for either antibody in both cell lines. Starting sample size=10,000 cells, $N = 3$ for each setting.

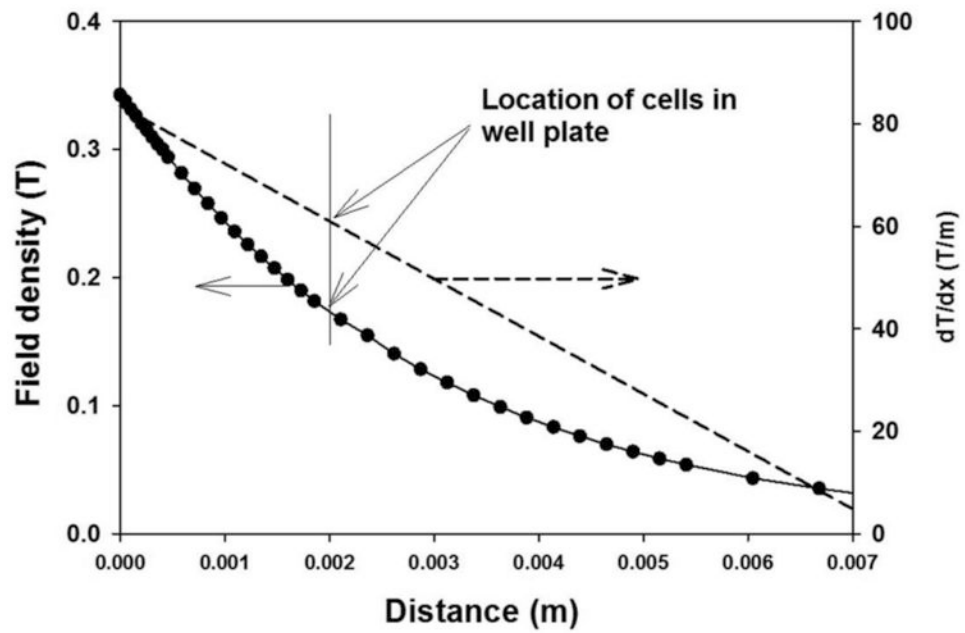


Figure 5. Magnetic field density (B , T) (left) and magnetic field density gradient (∇B , dT/dm) (right) as a function of perpendicular distance from the Dexter magnetic platform. Filled circles correspond to experimental measurement of the field density. The solid line corresponds to a second order fit to the data, and the dotted line the derivative of that 2nd order fit, representing ∇B . The vertical line corresponds to the distance that a monolayer of cells would be expected to be located at relative to the field (~ 2 mm).

Table 1

Maximum force acting on a cell with 20 MACSi beads attached in the 2D magnetic plate and the QMS cell sorter [36]. B = magnetic field, ∇B = magnetic field gradient.

Sorter	Estimated B (T)	Estimated ∇B (T/m)	Max force (pN)	Exposure Time (min)
Plate	0.175	60	120	3600
QMS	1.2	300	600	< 1

Author Manuscript

Author Manuscript

Author Manuscript

Author Manuscript